

# High power density supercapacitor electrodes of carbon nanotube films by electrophoretic deposition

Chunsheng Du and Ning Pan<sup>1</sup>

Nanomaterials in the Environment, Agriculture, and Technology (NEAT), University of California, Davis, CA 95616, USA

E-mail: [npan@ucdavis.edu](mailto:npan@ucdavis.edu)

Received 2 February 2006, in final form 18 September 2006

Published 6 October 2006

Online at [stacks.iop.org/Nano/17/5314](http://stacks.iop.org/Nano/17/5314)

## Abstract

Carbon nanotube thin films have been successfully fabricated by the electrophoretic deposition technique. The supercapacitors built from such thin film electrodes have a very small equivalent series resistance, and a high specific power density over  $20 \text{ kW kg}^{-1}$  was thus obtained. More importantly, the supercapacitors showed superior frequency response. Our study also demonstrated that these carbon nanotube thin films can serve as coating layers over ordinary current collectors to drastically enhance the electrode performance, indicating a huge potential in supercapacitor and battery manufacturing.

(Some figures in this article are in colour only in the electronic version)

## 1. Introduction

Carbon nanotubes (CNTs) are promising new materials for electrodes of electrochemical energy storage and conversion devices, owing to their unique internal structures, high surface area, low mass density, remarkable chemical stability and electronic conductivity. Consequently a wide range of their potential applications to electrochemical energy storage and conversion systems has been proposed in recent years, for example, as electrodes for supercapacitors [1–12], for Li-ion secondary batteries [13–17] and for hydrogen storage in fuel cells [18].

Supercapacitors, also called electrochemical capacitors or ultracapacitors, are able to provide a huge amount of energy in a short period of time, making them indispensable for surge-power delivery [19, 20]. It is worth noting that, in conventional supercapacitors, most of the surface area resides in micropores which are incapable of supporting an electrical double layer; this results in the worse frequency response: the energy stored in those carbon electrode materials can be withdrawn only at low frequencies. Recent efforts have been focused on the development of supercapacitors that have high

power density and improved frequency response [2, 21] for better performance and more demanding applications.

The maximum power density of a supercapacitor is given by  $P_{\max} = V_i^2/4R$  (where  $V_i$  is the initial voltage and  $R$  is the equivalent series resistance (ESR)) [22]. Accordingly, the key factors limiting the power density and frequency response of a supercapacitor are the internal resistivity of the electrode itself, the contact resistivity between the electrode and the current collector, and the resistivity of the electrolyte within the porous structure of the electrode [1, 21]. There have been several successful attempts at improving the power density and frequency response of supercapacitors. For example, Niu *et al* [21] reported that a better frequency response with a frequency ‘knee’ of about 100 Hz and a power density over  $8 \text{ kW kg}^{-1}$  were obtained by using free-standing mats of entangled multi-walled carbon nanotubes (MWNTs) as electrodes. An [1, 4] obtained high power density with single-walled carbon nanotubes while using polished nickel foil for lower contact resistivity and conducting a heat treatment at higher temperature to reduce the internal resistance of the carbon nanotube electrode. Yoon [10] lowered the contact resistivity by directly growing carbon nanotubes on metal current collectors using hot filament plasma enhanced chemical vapour deposition (HFPECVD). In our previous work [23], we have lowered the equivalent

<sup>1</sup> Author to whom any correspondence should be addressed.

series resistance (ESR) of electrodes significantly, owing to the coherent structure of the thin films fabricated using a highly concentrated colloidal suspension of carbon nanotubes. While being devoted to improve the performance of the supercapacitors made of CNTs, another more practical but just as important issue is the fabrication efficiency of such supercapacitors; there is still no viable method reported to prepare CNT-based electrodes with controlled quality in a large scale and in massive quantity.

We report here an electrode coated with an MWNT thin film prepared by the electrophoretic deposition (EPD) technique, which has the advantages of short formation time, simple apparatus, improved adherence of electrophoretically deposited coatings compared with dipped or sprayed coatings, and suitability for mass production [24]. The supercapacitors built from the EPD film electrodes offered an extremely small ESR, thus a high power density; and also exhibited superior frequency response. All of these make EPD a highly attractive route in fabricating CNT electrodes for high performance supercapacitors and other similar devices.

## 2. Experimental section

The multi-walled carbon nanotubes (MWNTs) used for this study were made via chemical vapour deposition (CVD), which has been described elsewhere [23]. Purified nanotubes were refluxed with concentrated boiling nitric acid for 12 h, and then washed with distilled water followed by rinsing with ethanol and drying at 60 °C. In a typical EPD experiment, 6 mg of refluxed MWNTs were dispersed in 60 ml of absolute ethanol by ultrasonication. In order to get a surface charge on the carbon nanotubes,  $10^{-5}$ – $10^{-4}$  mol of  $\text{Mg}(\text{NO}_3)_2 \cdot 6\text{H}_2\text{O}$  were added into the suspension as electrolyte for EPD. Two 5 mm diameter nickel foils were used as electrophoretic deposition (EPD) electrodes, and were put into the suspension and kept parallel. An upward deposition setup was used to separate EPD from sedimentation [25]. A dc voltage of 40–50 V was applied on the EPD electrodes and thus the charged carbon nanotubes were attracted towards the cathode. The EPD films were heated in a tube furnace at 500 °C for 30 min under a hydrogen environment, and then cut into small samples with dimensions 0.8 by 0.8 cm for further testing.

The purified carbon nanotubes were characterized by transmission electron microscopy (TEM; Philips CM 120), and the microstructures of the electrodes were investigated by high resolution scanning electron microscopy (SEM; FEI XL30-SFEG). For electrochemical measurement, a test cell of a capacitor (working potential: 1 V) was fabricated with 6 N KOH used as the electrolyte. A cellulose fibre filter paper immersed in the electrolyte was used as a separator placed between the two electrodes. The electrochemical behaviour of the supercapacitor was analysed in a two-electrode system using cyclic voltammetry (CV) and galvanostatic charge/discharge on a potentiostat/galvanostat (EG&G Princeton Applied Research, Model 263A), and electrochemical impedance spectroscopy (EIS) on a frequency response detector driving the EG&G 263A.

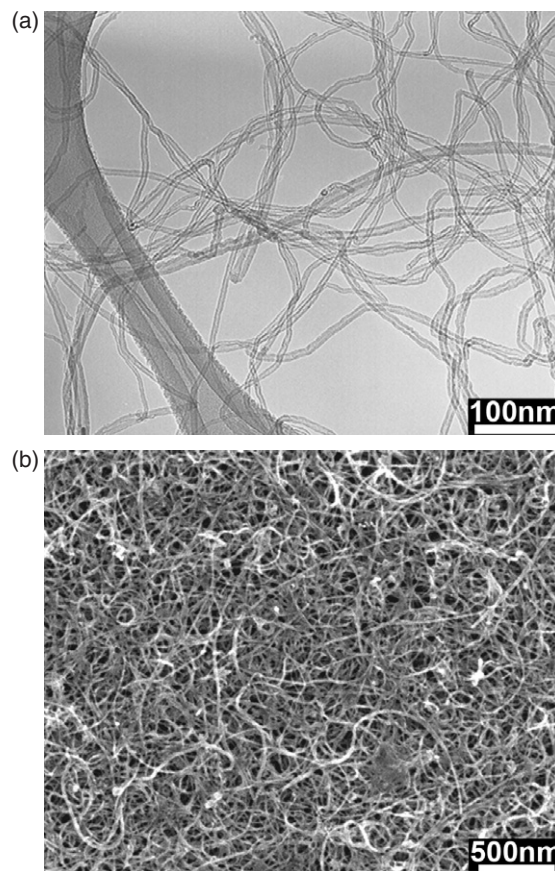


**Figure 1.** (a) TEM image of the purified carbon nanotubes; (b) SEM image of the EPD film.

## 3. Results and discussion

Figure 1 shows the TEM image of the purified carbon nanotubes used to fabricate the carbon nanotube thin films. The grown carbon nanotubes have very narrow diameter distribution, with average diameter of about 20 nm. The thermogravimetric experiment indicated that the purity of nanotubes was about 96%. An SEM image of the nanotube thin film grown by EPD is shown in figure 1(b). It can be seen that the film has a uniform pore structure formed by the open space between entangled nanotubes. Such an open porous structure with a high accessible surface area is unobtainable with other carbon materials, and enables easy access of the solvated ions to the electrode/electrolyte interface, which is crucial for charging the electric double layer.

The current response profile of the CV curves at a scan rate of  $50 \text{ mV s}^{-1}$  (figure 2(a)) is almost ideally rectangular along the time-potential axis, and the CV curves show almost mirror images with respect to the zero-current line, except for the small peaks at +0.9 to +1.0 V and -0.9 to 1 V, attributable to the redox reactions caused by the residual functional groups remaining on the nanotubes [8]. It should be noted that this peak gradually diminished due to the removal of those functional groups. Nevertheless, the CV curves still present a nearly rectangular shape, a clear proof of well developed capacitance properties. Even at a very high scan rate of  $1000 \text{ mV s}^{-1}$ , the CVs still retain their rectangular shape.

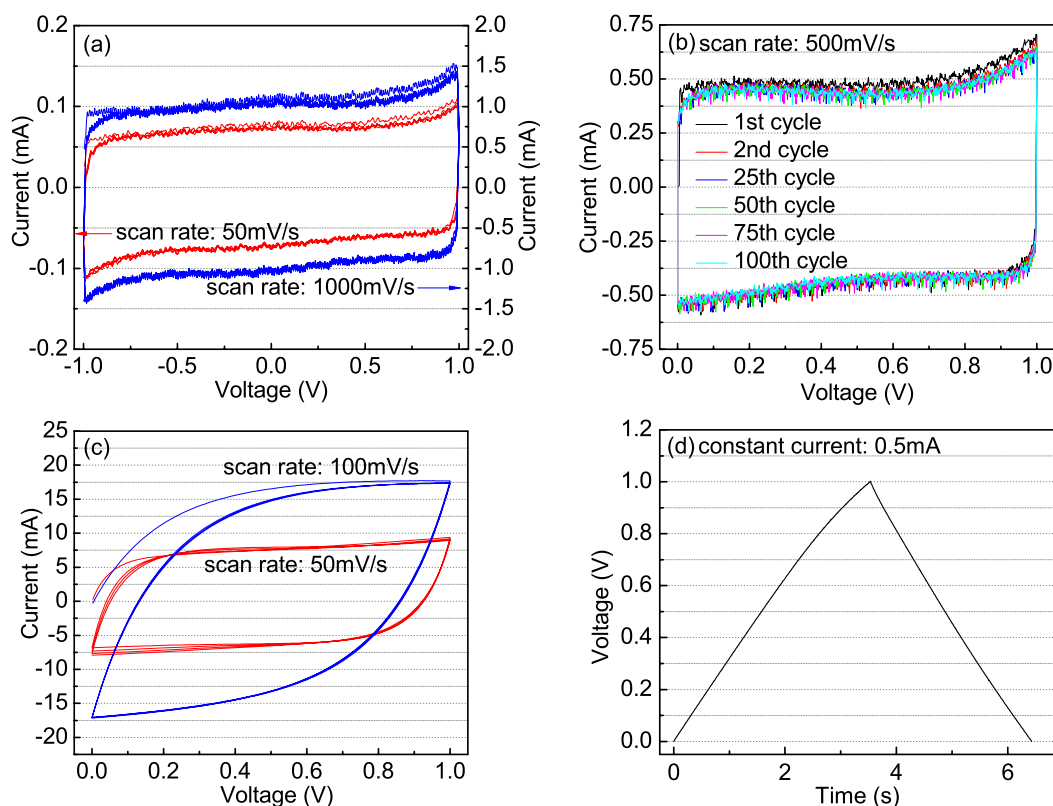


**Figure 2.** (a) CVs of the nanotube thin film supercapacitor cycled from  $-1$  V to  $+1$  V, (b) CVs of the nanotubes thin film supercapacitor cycled from  $0$  V to  $+1$  V for 100 cycles, (c) CVs of a conventional supercapacitor made of carbon particle thin films, and (d) charge/discharge curves of the nanotube thin film supercapacitor.

The excellent CV shape at such a high scan rate reveals a very rapid current response on voltage reversal at each end potential, and the straight rectangular sides represent a very small ESR of the electrodes and also the fast diffusion of electrolyte in the films [22]. We found that the shape of CV curves in the range  $-1$  to  $+1$  V is the same as that in the range  $0$  to  $+1$  V, so we chose to measure the CV curves in the  $0$  to  $+1$  V range in our further study. The capacitor was cycled for 100 cycles and no degradation was observed at all, as shown in figure 2(b). The capacitance calculated from the CVs is  $21 \text{ F g}^{-1}$ , and a power density of  $20 \text{ kW kg}^{-1}$  based on the active materials is easily obtained here. It should be noted that all of the data presented here were obtained from a real two-electrode system, and not from a half-cell or single electrode. This is important to note because most data in the literature are from the three-electrode system, which quadruples the values shown here [26, 27], and are sometimes overestimated [28]. An experimental comparison with a conventional supercapacitor made of carbon particle thin film electrodes was carried out, as shown in figure 2(c). Though the CVs of the supercapacitor made of carbon particle thin films at a scan rate of  $50 \text{ mV s}^{-1}$  are relatively close to rectangular shape, they showed a distorted shape at a scan rate of  $100 \text{ mV s}^{-1}$ . Clearly, the ESR in this conventional supercapacitor is much larger than that of the nanotube thin film supercapacitor.

A typical constant current charge/discharge curve of the nanotube thin film supercapacitor is shown in figure 2(d).

As can be seen, the  $E-t$  responses of the charge process show almost the mirror image of their corresponding discharge counterparts, and no IR drop was observed, again reflecting the small ESR of the electrodes.

More importantly, supercapacitors built from the EPD thin film electrodes also displayed superior frequency response. Figure 3(a) shows a complex-plane plot of the impedance of the supercapacitor. The impedance curve intersects the real axis at a  $45^\circ$  angle, which is consistent with the porous nature of the electrodes when saturated with electrolyte. The impedance plots can be divided into a high-frequency component (inclined at  $45^\circ$ ) and a low-frequency component (near vertical) with the transition point between the two regions being referred to as the ‘knee’ [2, 21]. The knee frequency denotes the maximum frequency at which capacitive behaviours is dominant, and is an indication of the power capability of a supercapacitor. Note that the ‘knee’ frequency in the impedance plot shown in figure 3(a) is about  $7560 \text{ Hz}$ , which suggests that most of its stored energy is accessible at frequencies as high as  $7560 \text{ Hz}$ . To the best of our knowledge, the highest reported knee frequency in other capacitors from CNT electrodes is  $100 \text{ Hz}$  [2, 21], while the knee frequency for most commercially available supercapacitors, including those specially designed for high power applications, is lower than  $1 \text{ Hz}$  [29]. Since a better frequency response means a better power performance, this great improvement in frequency response of our nanotube thin film electrodes by EPD constitutes a substantial advance in the rate of charge and discharge of the supercapacitor.

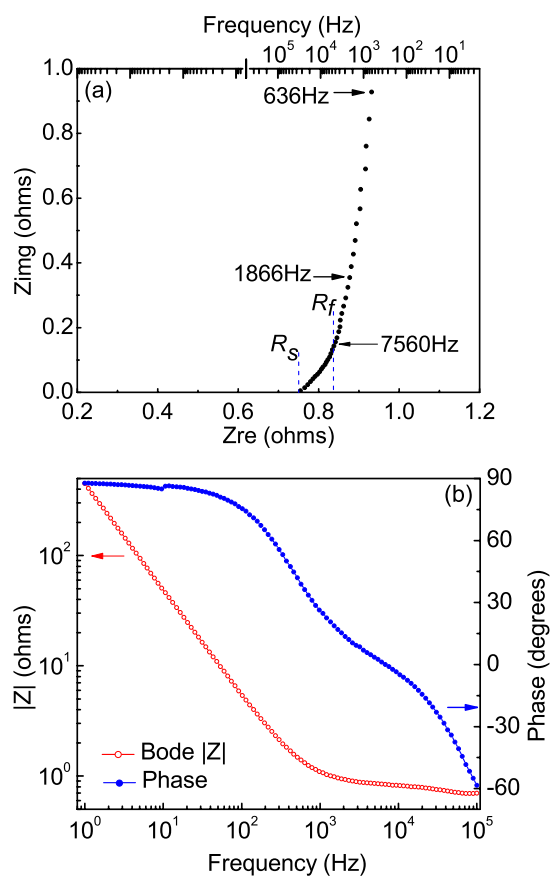


**Figure 3.** (a) Complex-plane impedance spectrum, and (b) Bode  $|Z|$  and Bode angle plots of the supercapacitor made of EPD thin film electrodes.

From the physics aspect, this superior frequency response of our supercapacitor is due to small ESR and the excellent electrolyte access to the thin films through its unique pore network formed by EPD. The EPD film is characterized as porous structures with significant volume of mesopores, thus enabling the excellent electrolyte access to the porous network in the film. In addition, the carbon nanotubes in the film form a highly conductive network, thus reducing the internal resistance within the thin film electrode itself. Furthermore, during the EPD process, all the nanotubes were driven by the electrical field, then uniformly deposited and compactly bonded to the nickel foil, providing a direct conductive path between the thin film electrode and the current collector; therefore the contact resistance is also significantly reduced. As can be seen in figure 3(a), the sum of the internal resistance of the thin film electrode itself and the contact resistance between the electrode and current collector,  $R_f$ , is only 830 m $\Omega$ ; therefore the contact resistance alone is even smaller (the KOH electrolyte resistance,  $R_s$ , is about 750 m $\Omega$  in this study). As proposed previously for other systems [24, 30, 31], the improved adhesion of the carbon nanotube film to the nickel foil in this study has likely resulted from the formation of magnesium hydroxide from magnesium ions at the surface of the EPD cathode (nickel foil), and these hydroxides could then hydrogen bond to the surfaces of the acid-oxidized nanotubes. The adhesion strength was further enhanced by our post-

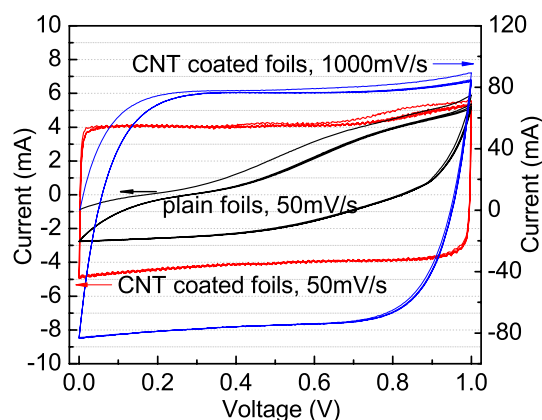


**Figure 4.** CVs of the supercapacitors from filtered carbon nanotubes mats while using different current collectors: black line—plain nickel foils as current collectors, at a scan rate of 50  $\text{mV s}^{-1}$ ; red and blue lines—CNT coated nickel foils as current collectors, at a scan rate of 50 and 1000  $\text{mV s}^{-1}$ , respectively.

deposition heat treatment in the hydrogen environment at 500  $^{\circ}\text{C}$ , as also proved by Russ *et al* [30]. Considering the strong adhesion and the high specific surface area of carbon nanotubes (thus the large contact area of nanotubes with the foil), efficient conducting paths between the nanotubes and the current collector are ensured, leading to a very small contact resistance of the electrode. Indeed, the EPD film electrodes did show a much better electrochemical performance than those prepared by direct deposit of a carbon nanotube suspension, evidenced by the rectangular CV curves even at a scan rate of 1000  $\text{mV s}^{-1}$  (figure 2(a)). In our previous report [23], the electrodes prepared by the direct deposition method only showed close-to-rectangular shaped CV curves at a scan rate of 500  $\text{mV s}^{-1}$ .

The changes of absolute impedance and phase angle as a function of frequency are shown in the Bode  $|Z|$  and angle plots for the EPD supercapacitor in figure 3(b). For frequencies up to 100 Hz, the phase angle is very close to 90 $^{\circ}$ , which again indicates that the device functions close to being an ideal capacitor.

In addition to being used directly as supercapacitor electrodes, the EPD films can also be used as a coating over other current collectors to reduce the contact resistance between the active materials and the current collectors. To demonstrate this concept, we prepared carbon nanotube mats by filtrating a suspension of purified MWNTs (without acid oxidation). These free-standing mats are much thicker compared to the EPD films and therefore are capable of outputting a much higher current. Figure 4 shows the CVs of the supercapacitors from the filtered mat electrodes while using different current collectors. When plain nickel foils were used as the current collectors, the CV curves at a scan rate of 50  $\text{mV s}^{-1}$  are very distorted loops. Clearly, there is a big contact resistance between the nanotube mats and the current collectors. However, when nickel foils coated with a very thin layer of carbon nanotubes were used as the current collectors, the CV curves show very nice rectangular shape at a scan rate of 50  $\text{mV s}^{-1}$ ; even at a very high scan rate of 1000  $\text{mV s}^{-1}$ , the CVs are still very close to rectangular shape, indicating that the ESR is very small due to the low contact resistance.

Since the electrodes used in this test were the same mats, the improved performance has to be attributed to the coated carbon nanotube layer on the nickel foils, which increased the contact surface area between the current collectors and the mats and also lowered the contact resistance due to the extremely strong bonding and direct conductive paths between the nanotubes and the nickel foils.

In conclusion, we have successfully fabricated MWNT thin film electrodes via the electrophoretic deposition technique. The supercapacitors built from these electrodes have exhibited a significantly small ESR, and a high specific power density. The supercapacitors also showed superior frequency response, with a frequency 'knee' more than 70 times higher than the highest reported knee frequency for supercapacitors. In addition, this carbon nanotube thin film can also act as a coating over ordinary current collector to decrease the contact resistance between the active materials and the current collector for improved performance. Owing to the nature and versatility of the EPD process, our current approach may provide a promising technique for massive fabrication of such CNT electrodes for various energy storage devices.

### Acknowledgments

Financial supports from UC Discovery Grant (ele03.10175) and EISG Program (03-28) are gratefully acknowledged.

### References

- [1] An K H, Kim W S, Park Y S, Choi Y C, Lee S M, Chung D C, Bae D J, Lim S C and Lee Y H 2001 *Adv. Mater.* **13** 497–500
- [2] Hughes M, Shaffer M S P, Renouf A C, Singh C, Chen G Z, Fray J and Windle A H 2002 *Adv. Mater.* **14** 382–5
- [3] Hughes M, Chen G Z, Shaffer M S P, Fray D J and Windle A H 2002 *Chem. Mater.* **14** 1610–3
- [4] An K H, Kim W S, Park Y S, Moon J M, Bae D J, Lim S C, Lee Y S and Lee Y H 2001 *Adv. Funct. Mater.* **11** 387–92
- [5] Liu C Y, Bard A J, Wudl F, Weitz I and Heath J R 1999 *Electrochem. Solid State Lett.* **2** 577–8
- [6] Barisci J N, Wallace G G and Baughman R H 2000 *J. Electroanal. Chem.* **488** 92–8
- [7] Diederich L, Barborini E, Piseri P, Podesta A, Milani P, Schneuwly A and Gally R 1999 *Appl. Phys. Lett.* **75** 2662–4
- [8] Frackowiak E, Metenier K, Bertagna V and Beguin F 2000 *Appl. Phys. Lett.* **77** 2421–3
- [9] Frackowiak E, Jurewicz K, Delpeux S and Beguin F 2001 *J. Power Sources* **97–98** 822–5
- [10] Yoon B J, Jeong S H, Lee K H, Kim H S, Park C G and Han J H 2004 *Chem. Phys. Lett.* **388** 170–4
- [11] Frackowiak E, Jurewicz K, Szostak K, Delpeux S and Beguin F 2002 *Fuel Process. Technol.* **77** 213–9
- [12] An K H, Jeon K K, Heo J K, Lim S C, Bae D J and Lee Y H 2002 *J. Electrochem. Soc.* **149** A1058–62
- [13] Claye A S, Fischer J E, Huffman C B, Rinzler A G and Smalley R E 2000 *J. Electrochem. Soc.* **147** 2845–52
- [14] Frackowiak E, Gautier S, Gaucher H, Bonnamy S and Beguin F 1999 *Carbon* **37** 61–9
- [15] Gao B, Kleinhammes A, Tang X P, Bower C, Fleming L, Wu Y and Zhou O 1999 *Chem. Phys. Lett.* **307** 153–7
- [16] Shin H C, Liu M L, Sadanadan B and Rao A M 2002 *J. Power Sources* **112** 216–21
- [17] Maurin G, Bousquet C, Henn F, Bernier P, Almairac R and Simon B 1999 *Chem. Phys. Lett.* **312** 14–8
- [18] Nutzenadel C, Zuttel A, Chartouni D and Schlapbach L 1999 *Electrochem. Solid State Lett.* **2** 30–2
- [19] Kotz R and Carlen M 2000 *Electrochim. Acta* **45** 2483–98
- [20] Burke A 2000 *J. Power Sources* **91** 37–50
- [21] Niu C M, Sichel E K, Hoch R, Moy D and Tennent H 1997 *Appl. Phys. Lett.* **70** 1480–2
- [22] Conway B E 1999 *Electrochemical Supercapacitor: Scientific Fundamentals and Technological Application* (New York: Kluwer Academic/Plenum Publisher)
- [23] Du C S, Yeh J and Pan N 2005 *Nanotechnology* **16** 350–3
- [24] Van der Biest O O and Vandeperre L J 1999 *Annu. Rev. Mater. Sci.* **29** 327–52
- [25] van Tassel J and Randall C A 2004 *J. Mater. Sci.* **39** 867–79
- [26] Mayer S T, Pekala R W and Kaschmitter J L 1993 *J. Electrochem. Soc.* **140** 446–51
- [27] Qu D Y and Shi H 1998 *J. Power Sources* **74** 99–107
- [28] Raymundo-Pinero E, Khomenko V, Frackowiak E and Beguin F 2005 *J. Electrochem. Soc.* **152** A229–35
- [29] Miller J R 1995 Battery-capacitor power source for digital communication applications: simulations using advanced electrochemical capacitors *Electrochemical Society Mtg (Oct. 1995)* (Chicago, IL: American Electrochemical Society)
- [30] Russ B E and Talbot J B 1998 *J. Electrochem. Soc.* **145** 1245–52
- [31] Siracuse J A, Talbot J B, Sluzky E and Hesse K R 1990 *J. Electrochem. Soc.* **137** 346–8